Simulating lake ice phenology using a coupled atmosphere-lake model at Lake Nam Co, a typical deep alpine lake on the Tibetan Plateau

Xu Zhou[1], Binbin Wang[1], Xiaogang Ma[2], Zhu La[3], and Kun Yang[2]

[1]State Key Laboratory of Tibetan Plateau Earth System and Resource Environment, Institute of Tibetan Plateau Research, Chinese Academy of Sciences, Beijing 100101, China
[2]Department of Earth System Science, Ministry of Education Key Laboratory for Earth System Modelling, Institute of Global Change Studies, Tsinghua University, Beijing 100084, China
[3]School of Ecology and Environment, Tibet University, Lhasa 850000, China

Correspondence to: Binbin Wang (wangbinbin@itpcas.ac.cn)

Abstract. Simulating the ice phenology of deep alpine lakes is important and challenging in coupled atmosphere-lake models. In this study, the Weather Research and Forecasting (WRF) model, coupled with two lake models, the fresh-water lake model (WRF-FLake) and the default lake model (WRF-CLake), was applied to lake Nam Co, a typical deep alpine lake located in the centre of the Tibetan Plateau, to simulate its lake ice phenology. Due to the large errors in simulating lake ice phenology, related key parameters and parameterizations were improved in the coupled model based on observations and physics-based schemes. By improving the momentum, hydraulic and thermal roughness length parameterizations, both the WRF-FLake and the WRF-CLake models reasonably simulated the lake freeze-up date. By improving the key parameters associated with shortwave radiation transfer process when lake ice exists, both models generally simulated the lake break-up date well. Compared with WRF-CLake without improvements, the coupled model with both revised lake models significantly improved the simulation of lake ice phenology. However, there were still considerable errors in simulating the spatial patterns of freeze-up and break-up dates, implying that significant challenges in simulating the lake ice phenology still exist in representing some important model physics, including lake physics such as grid-scale water circulation, and atmospheric processes such as snowfall and surface snow dynamics. Therefore, this work can provide valuable new implications for advancing lake ice phenology simulations in coupled models and the improved model also has practical application prospects in weather and climate forecasts.

1 Introduction

Alpine lake is one key land cover type on the Tibetan Plateau (TP). These lakes serve as a main water supply of the TP, i.e., the 'Asia water tower' [*Xu et al.*, 2008], with a total coverage of more than 47000 km[2] [*Zhang et al.*, 2019; *Zhang et al.*, 2014], which is about 2% the total area of TP. Therefore, alpine lakes play a crucial role in local and regional climate through thermal and hydrological cycles in the Earth system. For example, lakes, especially large lakes, can generally

enhance and/or change the temporal/spatial distributions of the precipitation over lakes and surroundings through both dynamic and thermal processes [*Dai et al.*, 2018b; *Su et al.*, 2020; *Wu et al.*, 2019; *Yang et al.*, 2022; *Yao et al.*, 2021; *Zhao et al.*, 2022]. An accurate simulation of lake climatic impacts can enhance the reliability of forecasting results in climate models. However, there are still large uncertainties in the parameterizations of the associated physical processes.

35 Lakes over mid-high latitudes undergo seasonal freeze-thaw cycles. Due to the large contrast in heat capacity associated with the large water storage per unit area, deep lakes often show significantly different ice phenology characteristics compared to shallow lakes and surrounding land areas. Many alpine lakes are deep lakes with average depths greater than 20 metres, such as Qinghai Lake, Nam Co, and Selin Co [*Guo et al.*, 2016; *Li et al.*, 2016; *Wang et al.*, 2009]. The ice phenology of alpine lakes can influence not only the lake water and energy budget, but also the seasonality of local and regional climates. For

40 example, lake freeze-up in cold season can maintain water levels by preventing evaporation losses in lakes [*Lei et al.*, 2018]. The surface evaporation of lakes will significantly increase during the cold ice-free period due to the strong turbulent mixing of lake water, which can provide appropriate moisture conditions for snowfall events.

The freeze-up date of a lake depends on the balance of energy storage. Turbulent heat fluxes play an important role in simulating the energy stored by lake water, and thus influence the freeze-up date [*Ma et al.*, 2022; *Zhou et al.*, 2023]. The

45 parameterizations of lake surface turbulent heat fluxes may have large uncertainties [*Wen et al.*, 2016], while the formulations of radiation processes at the water surface are relatively stable. Thus, the physical schemes of the heat fluxes need to be accurately parameterized in numerical models. One key parameter in simulating the turbulent heat fluxes is the roughness length, the parameterization of which plays an important role in accurately simulating the turbulent heat fluxes across the North American Great Lakes [*Deacu et al.,* 2012; *Charusombat et al.,* 2018]. It was also proven to have

50 significant influence on simulating the freeze-up date of Nam Co [*Ma et al.*, 2022]. The melting of lake ice mainly depends on solar radiation related processes [*Efremova and Pal'shin*, 2011; *Huang et al.*, 2022], especially the shortwave processes for ice and water, which are closely related to the albedo and the extinction coefficient [*Kirillin et al.*, 2012; *Li et al.*, 2021]. The absorption of the shortwave at the ice surface, deep ice, and water underneath can result in different ice thicknesses and freeze-up dates [*Zhou et al.*, 2023].

55 Offline lake models show considerable ability to simulate the seasonal freeze-up and break-up dates of alpine lakes [*Dai et al.*, 2018a; *Huang et al.*, 2019a; *Huang et al.*, 2019b; *Li et al.*, 2021]. However, regional climate and weather forecasts, as well as the lake effect can be achieved only through a coupled model. Therefore, the application and ability of coupled atmosphere-lake models for deep alpine lakes still needs to be further investigated, as highlighted in previous studies [*Su et al.*, 2020; *Wu et al.*, 2019; *Zhou et al.*, 2023]. It is more challenging for a coupled atmosphere-lake model to simulate the ice

60 phenology of alpine lakes, because for offline simulation, the atmospheric forcing is prescribed from observation or reanalysis data, which is a strong constraint on model performance and usually has fatal disadvantages. For example, the shortwave radiation above lake surface can be 100 W/m^{-2} stronger than that of the surrounding land due to the cloud hole effect [*Yao et al.*, 2023]. Thus, simulating lake ice phenology using a coupled model is necessary and important. Furthermore, a coupled model is more sensitive to key parameters and parameterizations, since the long-term integration will

65 increase the model errors through the two-way exchange of energy and water between atmosphere and lake surface [*Zhou et al.*, 2023].

Therefore, in this work, the Weather Research and Forecasting (WRF) model coupled with two lake models, the fresh-water lake (FLake) model [*Mironov*, 2008] and the simplified Community Land Model (CLM) lake model [*Gu et al.*, 2015], was applied to a typical deep alpine lake, Nam Co. Noting that *Zhou et al.* [2023] proved by empirically multiply a constant on

70 fraction velocity can better simulate the surface turbulent heat fluxes and ice phenology of Nam Co. However, such sensitivity method is lack of observation support. The current work is an extension of that work by revising key parameters and improving key parameterizations using observations and physics-based schemes to better simulate key lake energy related processes, for example, turbulent heat fluxes with ice-free conditions, solar radiation transfer with ice-on conditions. The main objectives are to improve the simulation of the lake ice phenology in the WRF model for deep alpine lakes and to

75 suggest important topics for further study in more accurately simulating the lake ice phenology characteristics in coupled atmosphere-lake models. This work is expected to provide an updated model version that can better modeling the lake related processes.

2 Study region and data

2.1 Study region

80 The target lake is Nam Co (Figure 1a), which is a typical deep lake located in the central TP at approximately 30.7°N, 90.6°E. It covers an area of more than 2000 km^2 and has an average depth of approximately 40 m [*La et al.*, 2016]. This value is calculated from the total water storage [*Zhang et al.,* 2016] divide by lake area. The deepest area locates at the center of the lake, with a maximum depth of about 100 m. A detailed map of lake bathymetry can be found in previous studies [*Huang et al.,* 2019; *Wu et al.,* 2023]. Under global warming, the lake water level has experienced a rapid increase since the 1990s due

85 to the increase in precipitation, and the growing water supplied by melting snow and glaciers within the basin [*Lei et al.*, 2014; *Lei et al.*, 2013; *Zhang et al.*, 2020].
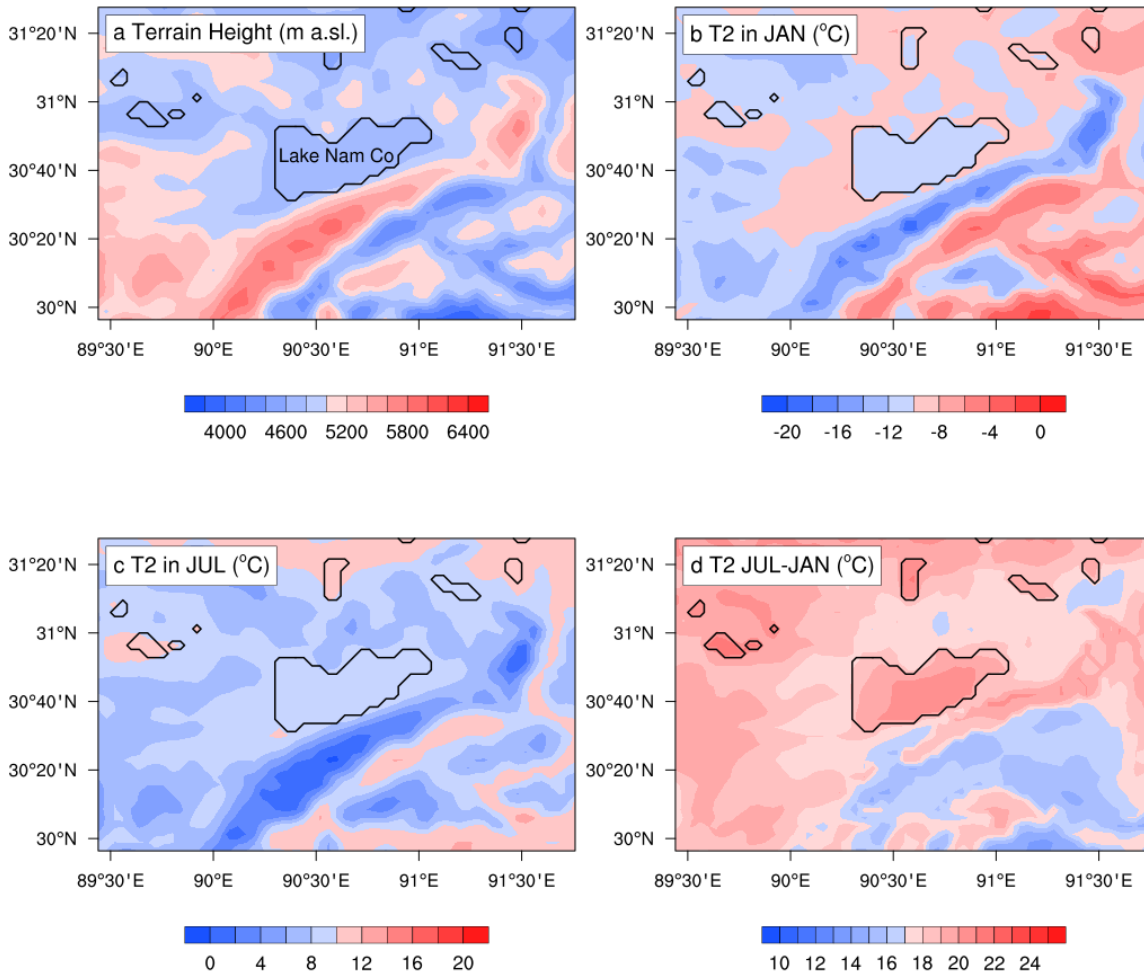
Figure 1: (a) The study region and the simulation domain of the current study, with Nam Co located in the centre; black contour lines denote the lake mask; colour shading denotes the terrain elevation (meters above sea level); the monthly averages of 2m air temperature (T2 in ℃) in (b) January and (c) July (colour shading) derived from default WRF simulation; and the difference of T2 (℃) between July and January (colour shading).

Seasonally, the study region undergoes large temperature variation with a cold monthly mean air temperature generally below 0 ℃ in January (Figure 1b) and a warm monthly mean air temperature generally above 0 ℃ in July (Figure 1c). Large air temperature difference between the two months can reach more than 22 ℃ (Figure 1d), indicating a strong seasonality, and thus the physical processes related with ice-water phase change may play an important role in the water and energy cycles within the study region. For example, compared with open water, frozen lake has much weaker evaporation and energy release to the atmosphere, and thus the climate effect of lakes will weaken simultaneously. Lakes over this region undergoes typical freezing and melting cycles.

4

2.2 Data

The lake water temperature (TW) data observed in Nam Co cover a period from November 2011 to June 2014 [*Wang*, 2020]. These data are the daily average water temperature data at different depths (3m, 6 m, 16 m, 21 m, 26 m, 31 m, 36 m, 56 m, 66 m and 83 m) and were obtained through field monitoring. The data were continuously recorded by deploying a water quality multi-parameter probes (CTD 90m, Germany) and temperature thermistors (VEMCO Minilog-II-T, Canada; accuracy: ±0.1 °C from −5 °C to 35 °C; resolution: 0.01 °C) in the water. The daily average water temperature was calculated based on the original observed data. In the current work, the TW was used for model evaluation. Only the data from the period of 1st July 2013 to 30nd June 2014 were used, because the station data after 1st July 2014 is not available due to the instrument damage.

The MODIS lake surface temperature (LST) product was used for comparison with the model results. The 0.05 ° Aqua and Terra daily datasets were used in the current study [*Wan et al.*, 2015]. For a fair comparison, the MODIS data were interpolated to the model grid by the area weighted method. Due to the contamination by clouds, MODIS has missing observations at a considerable number of pixels. Thus, the mean LSTs were calculated and compared with those from each simulation. For quality control, the LSTs with a fraction of missing observations larger than 90% were removed. Nonetheless, there were still some outliers especially for night time data. Additionally, the land-water mixed pixels (the nearest two pixels to land) in MODIS were excluded and a total of 1574 grid points were used.

ERA_interim reanalysis data [*Dee et al.*, 2011] from the European Centre for Medium-Range Weather Forecasts (ECMWF) was used for model initial and lateral boundary forcing conditions. It was developed based on the Integrated Forecasting System (IFS) model assimilating multisource observations. This data has a resolution of approximately 80 km (T255 spectral) on 60 vertical levels from the surface up to 0.1 hPa.

3 Model description and setup

3.1 WRF model and model setup

In this study, two lake models were used in the coupled atmosphere-lake model to demonstrate the universality of the revisions in parameterization schemes in improving the simulation of lake ice phenology characteristics. One is the FLake model and another one is the simplified CLM lake model. These two model are coupled with WRF and defined as WRF-FLake and WRF-CLake hereafter. The default WRF was developed by NCAR. It is a nonhydrostatic model with multiple schemes in the planetary boundary layer, the land surface model, the cloud microphysics, the cumulus convection, the orographic drag. In this study, WRF3.9 [*Skamarock et al.*, 2008] was applied to the TP region.

The two lake models have been coupled with WRF in a one-dimension way, i.e. no horizontal water flow is simulated. In the coupling strategy, a grid point with 50% lake cover is defined as a lake point. At each time step, lake models are driven by atmospheric forcing including air temperature, pressure, humidity, wind, short wave and long wave radiation, precipitation

and reference height (height of first atmospheric layer). While the lake models feedback momentum, sensible heat and latent heat fluxes.

Figure 1a shows the simulation domain, covering Nam Co and the surrounding land. The WRF model setup is generally consistent with *Zhou et al.* [2023], with a horizontal grid spacing of 0.04º (approximately 4.5 km), which is identified as convection-permitting. The coupled modes were run with a time step of 10 seconds. There are 116 lake grid points in the model. The lateral boundary conditions were provided at six hourly intervals. The simulations were performed for two years from 1st July 2013 to 30th June 2015. The lake water temperature in the coupled model was initialized at 00:00 on 1st July 2013 using MODIS observations. The water temperature at the first layer was set to MODIS observed values, while the water temperature at the other layers is linearly interpolated with depth under the assumption that the water temperature at the deepest layer is equal to 3.5℃ (the temperature at maximum water density). The other variables in the coupled model are initialized by ERA_interim data at the same time. Based on previous studies over the TP, a turbulent orographic form drag scheme was used to represent the subgrid orographic drag [*Zhou et al.*, 2017; *Zhou et al.*, 2021], the Dudhia scheme [*Dudhia*, 1989] and the RRTM [*Mlawer et al.*, 1997] were used for shortwave and longwave radiation transfer, the Modified Thompson scheme [*Thompson et al.*, 2008] was used for the microphysics, the Noah-MP [*Niu et al.*, 2011; *Yang et al.*, 2011] was used for the land surface processes, and the Mellor–Yamada–Janjic turbulent kinetic energy scheme [*Janjic*, 2001; *Mellor and Yamada*, 1974] was used for the planetary boundary layer.

Three experiments were designed in the current study. One used the WRF coupled with the default lake model without revisions of key lake parameters and parameterizations, which was defined as the control run (WRF-Ctrl). The other two used WRF coupled with the revised FLake model and revised default lake model, defined as WRF-FLake run and WRF-CLake run. The unrevised version of the WRF-FLake model was not selected as a control run because it had difficulties simulating the ice phenology characteristics, i.e. a considerable number of lake grid points never freeze-up, and/or never break-up after freeze-up [*Zhou et al.*, 2023].

3.2 Lake models and model setup

FLake is a freshwater model developed by *Mironov* [2008]. It is not designed with explicit fixed depth layers. There is an upper mixed layer and a thermocline layer in which the water temperature is parameterized by self-similarity theory. One key feature of FLake is that the mixed layer depth is parameterized by diagnosing the water stability conditions, which is different from the finite difference model in which the energy exchange is parameterized by a turbulent mixing ratio. FLake was coupled with WRF by *Zhou et al.* [2023] to perform sensitivity studies of key physical processes in simulating lake ice phenology. This study used the same version.

The other lake model is the default one in WRF, which is a simplified version of the CLM lake model. It is a finite differential model that was originally designed for shallow lakes. It has ten vertical layers and the water turbulent mixing

ratio is empirically set to a constant between the layers. The CLM lake model is simplified and coupled with WRF by *Gu et al.* [2015] to describe lake processes in WRF model.

165 Previous studies have shown that using the default settings in lake models can lead to considerable errors in the simulations [*Huang et al.*, 2019a; *Ma et al.*, 2022; *Zhou et al.*, 2023]. Thus, some key parameters and physical schemes were revised based on previous studies. For both lake model setups in the coupled model, the lake depth was set to the average value of 40 m for all lake grid points, which was consistent with the offline lake model simulations by *La et al.* [2016]. Thus, to save computational expense, their simulation results were used to initialize the lake water temperature in the coupled model.

170 Noting that both lake models used in the current study are one-dimensional models, no horizontal water flow is simulated in the coupled model. Such a model setup is a general way for modeling lake processes in a climate model, such as Community Earth System Model (CESM), Consortium for Small-scale Modelling (COSMO), as well as WRF model. The setup of following parameters is based on observation. The water extinction was set to 0.12 according to *Wang et al.* [2009] and *Huang et al.* [2019a]. The temperature at maximum water density was set to 3.5°C according to *Wang et al.* [2019b] and *Wu*

175 *et al.* [2019].

3.3 Model improvements and limitations

In the Default WRF-CLake model, the momentum, hydraulic and thermal roughness lengths were set to constant values of 0.001. In the default FLake model, the roughness length for momentum (z_{0m}) is parameterized as follows:

$$z_{0m} = \alpha \times \frac{u_*^2}{g}$$

180 (1)

where α is the Charnock number calculated by $\alpha = 0.0012 + 0.7 \times (1/1000 \times (u^2)/g)$, u is the surface wind speed; u_* is the surface friction velocity in m/s; $g = 9.8$ m/s^2 is the gravitational acceleration constant. Then, the hydraulic roughness length z_{0q} is further parameterized as follows:

$$z_{0q} = z_{0m} \times \exp\left(-C_k \times \left(4.0 \times \left(\frac{u_*^3}{g \times v}\right)^{0.5} - 4.2\right)\right) \tag{2}$$

185 where $C_k = 0.4$ is the Von Karman constant; v is the kinematic viscosity of air. And thermal roughness length z_{0h} is further parameterized as follows:

$$z_{0h} = z_{0m} \times \exp\left(-C_k \times \left(4.0 \times \left(\frac{u_*^3}{g \times v}\right)^{0.5} - 3.2\right)\right) \tag{3}$$

The above formulation is used in *Zhou et al.* [2023], which introduced large model errors in simulating lake ice freeze-up time. Because such a parameterization simulated too weak turbulent heat fluxes, which controls the lake water energy

190 balance. Empirically, these fluxes have too enlarged 1.5 times to improve the model performance. Nevertheless, such eempirical method lacks physical basis and is model dependent. In the current study, differently from such methods, an observation-based roughness length scheme for open water [*Wang et al.*, 2019a] was used for both WRF-CLake and WRF-

FLake, which have been proven to better simulate the heat fluxes and lake freeze-up date in WRF-CLake [*Ma et al.*, 2022]. z_{0m} is parameterized as follows:

195 $$z_{0m} = \alpha \times \frac{u_*^2}{g} + R_r \times \frac{\nu}{u_*} \qquad (4)$$

where $\alpha = 0.031$, $R_r = 0.54$, for; These two parameters are calibrated using field observations at lake Nam Co [*Wang et al.*, 2018]; ν is the kinematic viscosity of air; u_* is the surface friction velocity in m/s; $g = 9.8$ m/s^2 is the gravitational acceleration constant; and $R_e = u_* z_{0m}/\nu$ is the roughness Reynolds number. Then, the hydraulic and thermal roughness lengths z_{0q} and z_{0h} are further parameterized as follows:

200 $$z_{0q} = z_{0h} = z_{0m} \times \exp(-2.67 \times R_e^{0.25} + 0.57) \qquad (5)$$

where $R_e = u_* z_{0m}/\nu$ is the Reynolds number.

In Default WRF-CLake model, the division of the vertical layers of lake is four [*Ma et al.*, 2022]. In the current work, to better simulate the lake ice break-up date, the division of the vertical layers of the lake in WRF-CLake was revised to ten layers according to CLM4.5. During freeze-up, if the ice is covered with snow, then the lake surface albedo will be set to the

205 snow albedo. The default ice albedo in WRF-CLake is 0.6. In the current study, it was set to 0.55 with the consideration that 0.5-0.6 is the most distributed ranges of albedo observations for the Lake Nam Co, as investigated in *Li et al.* [2018]. In WRF-FLake, the albedo α is parameterized by the ice surface temperature as follows:

$$\alpha = \alpha_{max} - (\alpha_{max} - \alpha_{min})\exp(-95.6(T_f - T_s)/T_f) \qquad (6)$$

where α_{max} and α_{min} are the maximum and minimum ice albedo, respectively, $T_f = 273.15$ is the temperature at the

210 freezing point, and T_s is the ice surface temperature. In *Zhou et al.* [2023], the default values of α_{max} and α_{min} were set to 0.2 and 0.1 respectively, with the consideration of ice albedo variance under snow-free conditions. Nevertheless, the value of 0.2 is too small under all conditions (when snow often appears), as observed from satellite [*Li et al.*, 2018]. Therefore, in the current study, α_{max} is revised to 0.75 based on satellite observation [*Li et al.*, 2018]. In their study, the occurrence of maximum albedo during ice-on season at Nam Co is no more than 0.8 based on MODIS data. Such treatment of lake surface

215 albedo directly takes into account the snow influence on lake surface albedo. Therefore, we can make sure that the modeled snow fall biases will not directly bring uncertainties in simulating the lake processes. Over the complex terrain region, precipitation fall has been a great challenge and it is very difficult to correctly simulate precipitation amount. In TP, there is a systematic over estimation of precipitation in climate models [*Gao et al.,* 2015; *Su et al.,* 2013]. Additionally, considering the absorption of shortwave radiation at the ice surface is also an important parameter, it is revised to 0.65 according to a

220 sensitivity study similar to that in *Zhou et al.* [2023]. In the sensitivity study, all the simulations are initialized at the 1st January 2014, a few days before lake freeze-up, which make sure the lake water thermal status and the freeze-up dates are correct at the initial stage. Before freeze-up, the lake water is fully mixed and a uniform temperature initialization is reasonable. With an ice surface absorption ratio of 0.65, the model shows the best performance in simulating lake ice break-up date compared with other values (0.5, 0.55, 0.6, 0.7, and 0.75).

3.4 Calculation of lake freeze-up date and break-up date

Freeze-up date at each grid point is defined as the first day when lake ice occurs and ice-free days never occur in the following 20 days at this grid point, while break-up date at each grid point is defined as the first day when ice-free occurs after 20 ice-on days at this grid point. The freeze-up duration at each grid point is defined as the number of days with continuous ice cover at this grid point. It is derived from break-up date minus freeze-up data. Within each model grid point, there are 16 (4×4) co-located MODIS pixels. Thus, for the calculation of freeze-up date and break-up date by MODIS, the maximum LST in each grid point is selected from the co-located 16 MODIS pixels. The reason of using maximum LST rather than an average is that MODIS data may be contaminated by cloud top temperature, which could be much colder than real lake surface temperature. Additionally, such a treatment can preserve as much satellite information to maintain maximally continuous time series within the grid points. Even though, there are freeze-up date and break-up date in a considerable number of model grid points that are still cannot be effectively calculated due to too much missing observations in MODIS. The number of lake grid points with missing values are even larger when calculating the freeze-up durations by subtracting the break-up date and freeze-up date.

Treating the lake as a whole, the lake freeze-up date and lake break-up date is calculated based on lake frozen fraction. The lake frozen fraction is defined as the ratio of the number of ice-on grid points to all grid points. The lake freeze-up date is defined as the first day when the lake frozen fraction reaches 90% and does not fall below this threshold for 20 consecutive days, while the lake break-up date is defined as the first day when lake frozen fraction falls below 90% and never exceeds this threshold for 20 consecutive days. Lake freeze-up duration is derived from lake break-up date minus lake freeze-up date.

4 Results and analysis

4.1 Surface heat flux and water temperature

Previous studies show that there are large uncertainties in simulating turbulent heat fluxes in lake models [*Wen et al.*, 2016]. Additionally, turbulent heat fluxes play key roles in simulating the lake water temperature and lake freeze-up date [*Ma et al.*, 2022; *Zhou et al.*, 2023]. In contrast, other energy components at the lake surface are relatively more reasonably simulated due to reliable observations of related parameters. For example, regarding shortwave and longwave radiation, the albedo for open water is approximately 0.08 and the emissivity is approximately 0.98. These two key parameters have low uncertainties and can be accurately estimated. Therefore, only the simulated turbulent heat fluxes and water temperature were investigated in this section.

To demonstrate the effects of model improvements. Figure 2 shows the differences in daily mean sensible heat and latent heat derived from WRF-FLake and WRF-CLake minus WRF-Ctrl at Nam Co averaged over all lake grid points. Compared with WRF-Ctrl, both WRF-FLake and WRF-CLake show quite smaller differences in simulating the sensible heat for ice-free periods (Figure 2a), while they show considerable larger negative differences in simulating the latent heat for ice-free

periods especially within approximately one month before ice-on (Figure 2b), indicating that the LH is more sensitive to the improvements in the hydraulic and thermal roughness lengths parametrizations as introduced in section 3.2. The improved model WRF-FLake and WRF-CLake show quite good agreement with each other, because both models used the same parameterizations of momentum and thermal roughness lengths (Section 3.2). Both WRF-FLake and WRF-CLake obviously
260   show larger sensible heat and latent heat in November-December than WRF-Ctrl due to the early freeze-up in WRF-Ctrl model. The differences in sensible heat and latent heat at the initial stages of ice-on between the two improved models could be associated with the inconsistency in the freezing status of specific grid points between the two simulations. Additionally, other thermal processes (such as water turbulent mixing) also play certain roles and caused different model performances in simulating sensible heat, latent heat, and lake freeze-up time. Obviously, the smaller latent heat during ice-free periods in
265   both WRF-FLake and WRF-CLake simulations leads to a weaker water energy release, resulting in a late freeze-up.

The sensible heat and latent heat control the atmosphere-lake energy exchange and lake water energy storage, and thus influence the lake freeze-up date [*Ma et al.*, 2022; *Zhou et al.*, 2023]. In the following, the LST and water temperature profiles are compared with MODIS and station observations, respectively.
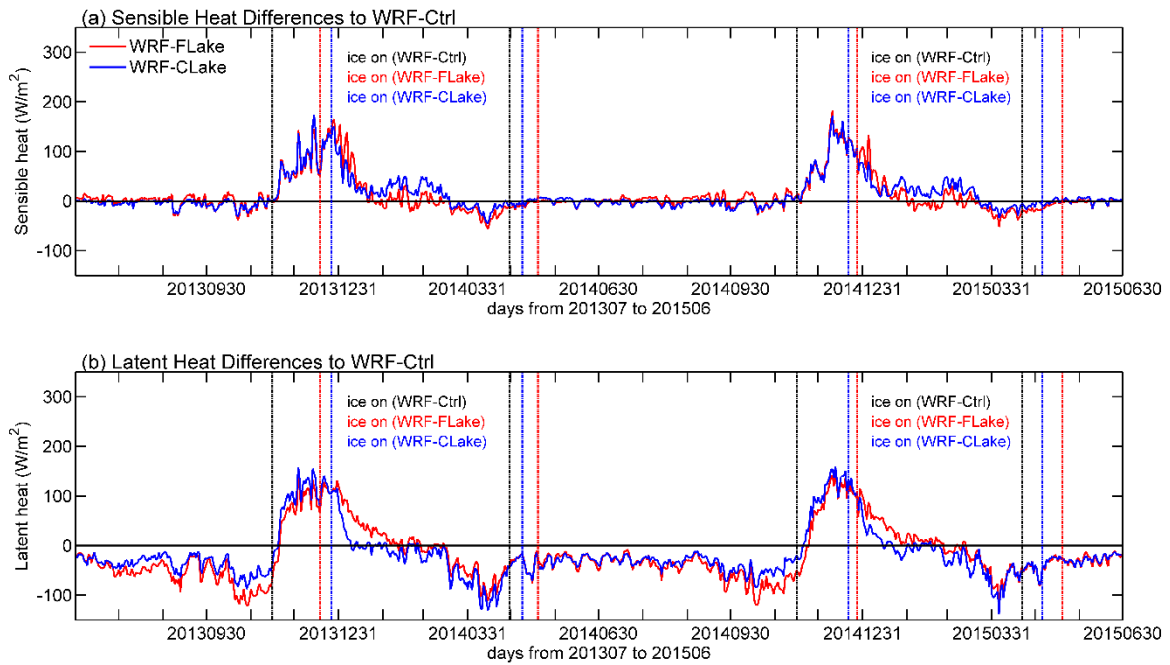
270

Figure 2: Differences in the daily mean (a) sensible heat and (b) latent heat simulated derived from WRF-FLake and WRF-CLake minus WRF-Ctrl at Nam Co averaged over all lake grid points for the study period. The vertical lines show the first/last days of ice occurrences in each simulation (black: WRF-Ctrl; red: WRF-FLake; blue: WRF-CLake).

275   Figure 3a shows the time series of mean LST biases (averaged over the grid points with MODIS observation) in each simulation (WRF-Ctrl, WRF-Flake, and WRF-CLake minus MODIS) for the study period. The biases are derived from WRF-Ctrl, WRF-Flake, and WRF-CLake runs minus MODIS. WRF-Ctrl obviously show cold biases during ice-free periods. These cold biases (for example in September and October) are alleviated in both the WRF-FLake and the WRF-CLake runs. Considering the uncertainties in the MODIS products, that is, there are obvious unreliable underestimations of night time

280   LST for alpine lakes including Nam Co [*La et al.*, 2022], slight warmer biases in LST are expected during ice-free periods as showed in the WRF-Flake and WRF-CLake runs in Figure 3a. Larger cold biases in WRF-Ctrl occurs in November-December due to the early ice-on, which is significantly improved in the WRF-FLake and the WRF-CLake runs. At the time of early ice-on in these two runs, the simulated LST also show cold biases. The reason could be that for MODIS, only ice-free pixels were averaged because the freeze-up pixels were hard to distinguish between lake surface or cloud top, which

285   also explains the continuous missing observations of MODIS during lake freeze-up. Therefore, the LST during early ice-on stage is logically incomparable between the model simulations and MODIS. Figure 3b shows the differences in the daily mean LST (averaged over all grid points) derived from WRF-FLake and WRF-CLake minus WRF-Ctrl for the study period. WRF-FLake and WRF-CLake runs obviously have warmer LST during ice-free period, which can be explained by the stronger cooling effect due to the larger LH release as shown in Figure 2b. The largest LST differences in WRF-FLake and

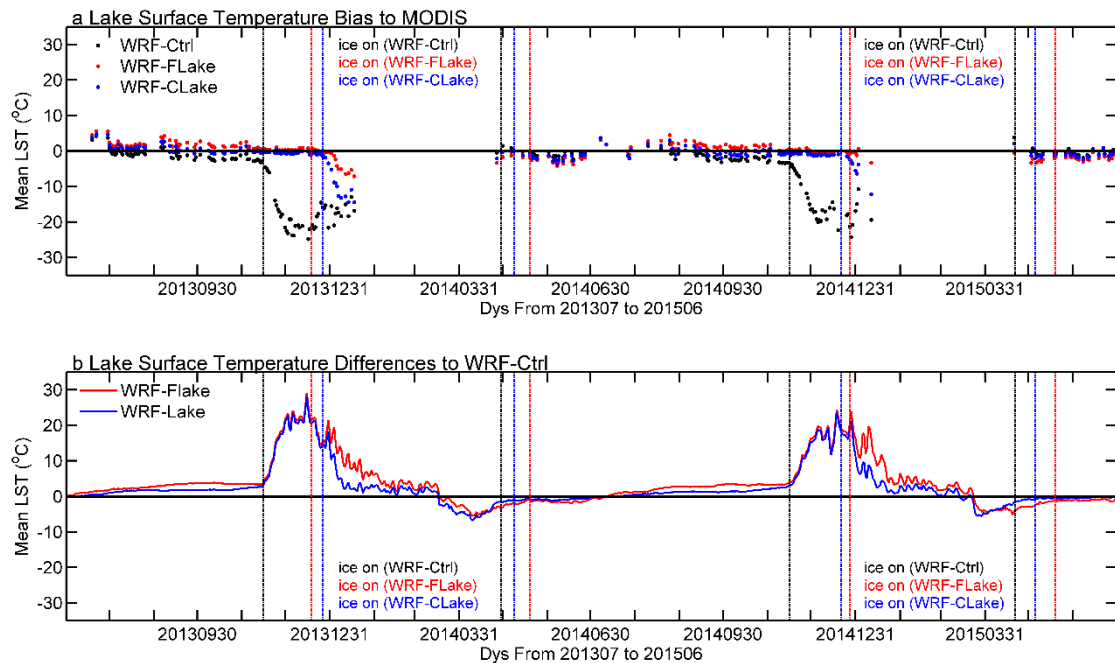290   WRF-CLake in November-December are caused by the early ice-on in the WRF-Ctrl.

Figure 3: (a) The biases in daily mean LST to MODIS in each simulation (black: WRF-Ctrl; red: WRF-FLake; blue: WRF-CLake) for the study period, and (b) the differences in the daily mean LST derived from WRF-FLake and WRF-CLake

11

minus WRF-Ctrl for the study period. The biases are derived from WRF-Ctrl, WRF-Flake, and WRF-CLake runs minus
295 MODIS. The differences are derived from WRF-Flake, and WRF-CLake runs minus WRF-Ctrl run. The vertical lines show
the first/last days of ice occurrences in each simulation (black: WRF-Ctrl; red: WRF-FLake; blue: WRF-CLake).

Figure 4 shows the observed and simulated lake water temperature profiles. Only the data from the period of 1st July 2013 to
30nd June 2014 were used, because the station data after 1st July 2014 were not available due to instrument damage. All the
300 simulations can generally simulate the seasonality of the water temperature with the maximum occurring in August-
September, and the minimum occurring in winter and early spring. Consistent with the investigation in *Wang et al.* [2019b],
obvious water stratification lasts from July to late October, while the water body is sufficiently mixed after that time until
May of the next year (Figure 4a). During the ice-on period, the thermal structure of the water column is weakly stratified
rather than mixed [*La et al.*, 2021]. The stratification characteristics in the simulations generally agree well with the
305 measurements (Figure 4b-c). Additionally, the mean bias and root mean square error (RMSE) are calculated (Figure 4d-e).
The WRF-Ctrl and WRF-CLake runs show cold biases, especially at shallow layers, while WRF-FLake has smaller mean
bias errors (Figure 4d). By revising key parameters and improving key parameterizations of lake models (as in section 3,2
and section 3.3), the cold biases can be effectively alleviated. The RMSE in WRF-FLake is larger at deep layers, indicating a
worse performance, and vice versa at shallow layers (Figure 4e). The mean bias in WRF_FLake is smaller than that in WRF-
310 Ctrl and WRF-CLake, while the RMSE is larger for some layers. This could be associated with the differences in seasonal
variation in the LST between the models and observations. That is, WRF-FLake (Figure 4b) is much warmer in summer and
colder in winter than is WRF-CLake (Figure 4c) compared with the observations (Figure 4a). When calculating the mean
bias, the more extreme warm bias and cold bias in WRF-Flake compensate each other. Generally, the errors in simulating the
lake water temperature are at reasonable scales compared with offline lake model simulation results in other studies [*La et al.*,
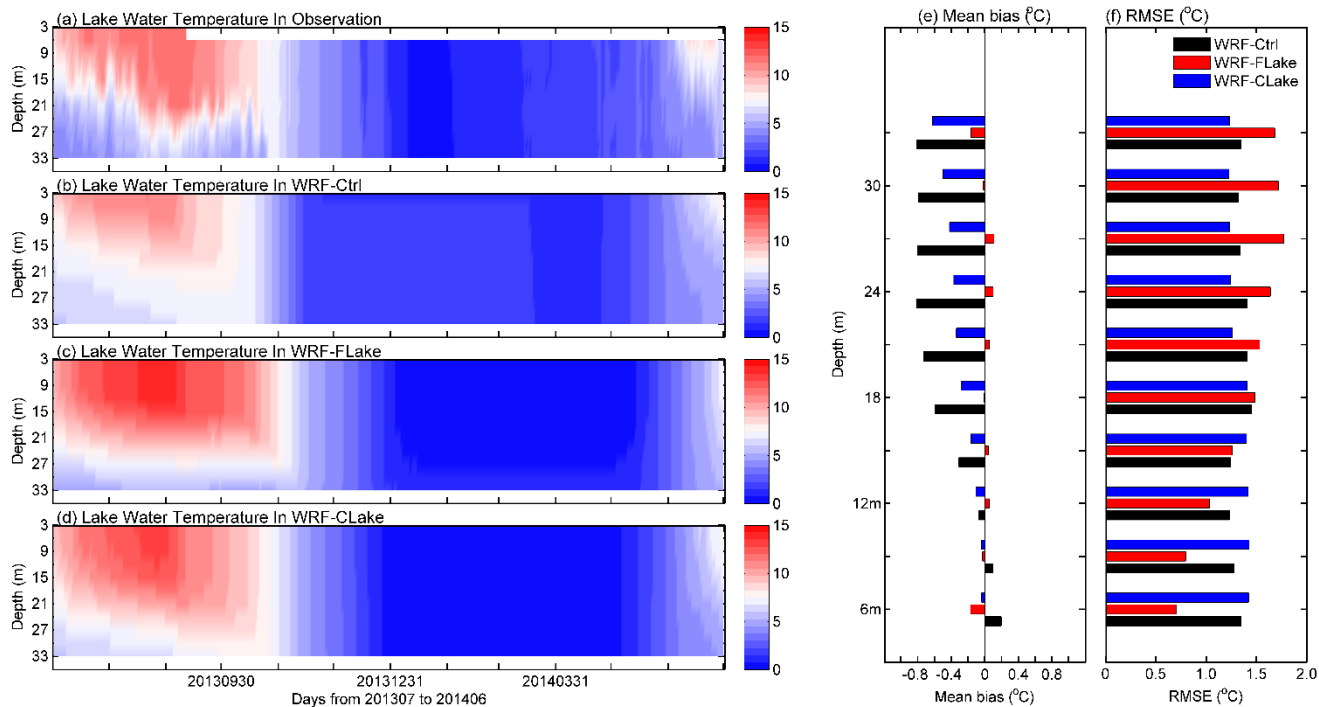315 2016; *Huang et al.*, 2019], which show RMSEs within the intervals of 1.0-2.5 °C and 1.8-2.4 °C.

Figure 4: Lake water temperature profiles in (a) station observations and each simulation (b: WRF-Ctrl, c: WRF-FLake and d: WRF-CLake) for the period of 1ˢᵗ July 2013 to 30ⁿᵈ June 2014, and (e-f) error metrics (mean bias and RMSE) at different depths.

4.2 Lake ice phenology characteristics

In this section, the simulated lake ice phenology is investigated, including the lake frozen fraction, ice thickness, freeze-up and break-up dates of the lake as a whole and for each lake grid, as well as the freeze-up duration. Following the method in *Zhou et al.* [2023], the ice phenology of lake Nam Co as a whole is investigated, including the frozen fraction, the mean ice thickness, and the penetrated shortwave radiation at the ice surface. Figure 5a shows the frozen fraction and mean ice thickness of Nam Co in each simulation. Based on MODIS, Nam Co generally freezes in January and breaks in late April (Figure 5a). For seasonality of lake ice phenology, both the WRF-FLake and the WRF-CLake runs generally show good agreement with MODIS, while WRF-Ctrl shows too-early freeze-up and break-up dates (Figure 5a). For ice thickness, WRF-FLake simulates thicker ice than WRF-CLake, with maximum thicknesses of approximately 0.5 m and 0.4 m, respectively (Figure 5b). The reason could be attributed to more penetrating shortwave radiation at the ice surface (Figure 5c), and this part of the energy is more effective in contributing to ice melting in the model as interpreted by *Zhou et al.* [2023]. Compared with these two runs, WRF-Ctrl has much smaller ice thickness, which maintains a constant thickness during the main freeze-up period. This is because the thickness of the second layer was set to 4.0 m by default, which is too deep and difficult to freeze. Additionally, the lake freeze-up and break-up dates, and freeze-up durations derived from each simulation

13

are compared with those from MODIS, as shown in Table 1. Generally, WRF-Ctrl shows more than one month earlier

335 freeze-up and break-up dates than MODIS, while both revised models simulate the lake freeze-up and break-up dates with

acceptable accuracy (errors smaller than 11 days), except for the break-up date in winter of 2014-2015 in WRF-CLake

(Table 1). WRF-Ctrl shows too long freeze-up durations, which are effectively reduced in both WRF-FLake and WRF-

CLake runs, though with too short freeze-up durations in WRF-CLake (Table 1). This result indicates that, regarding lake

freeze-up and break-up dates, the performances of WRF-Flake and WRF-CLake were significantly improved by revising key

340 parameters and improving key parameterizations in lake models.
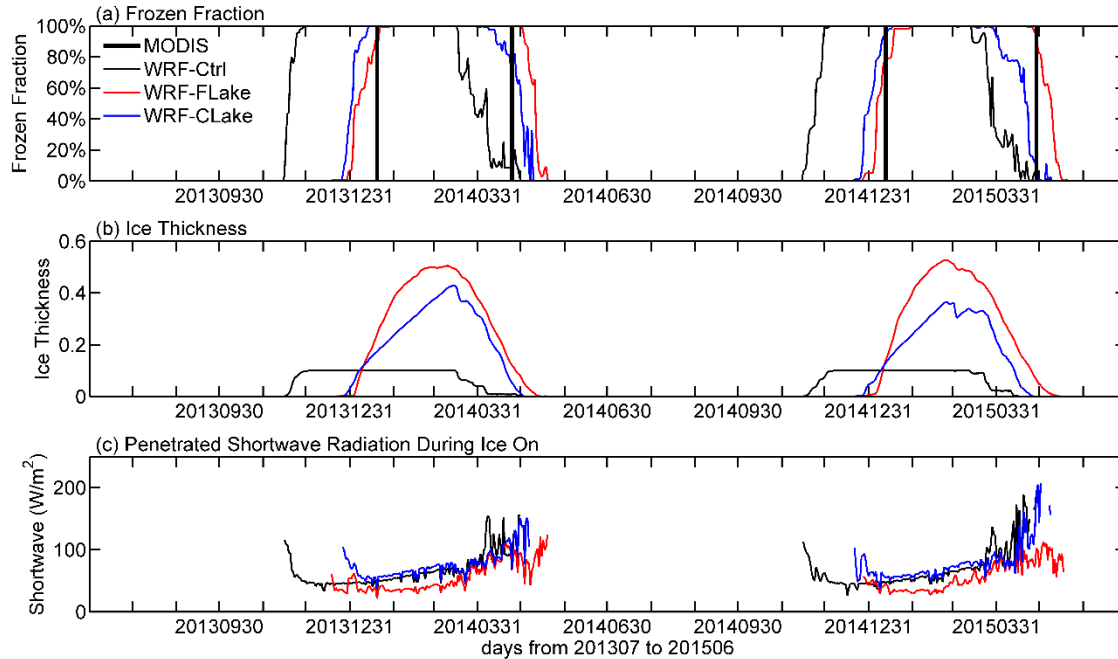
Figure 5: (a) Lake frozen fraction, (b) ice thickness, and (c) penetrated shortwave radiation (during the ice-on period) in each simulation. The vertical bold straight line indicates the freeze-up date and break-up date derived from MODIS.

345

Table 1: The comparisons of lake freeze-up dates, lake break-up dates and lake freeze-up durations (days) between each simulation and MODIS; the values indicate the number of days since 1st July of the corresponding year; the values in in parentheses indicate the errors of each simulation to MODIS; the Julian days of the freeze-up dates and break-up dates are provided for MODIS. Bold indicates a best performance.

	Freeze-up date	Break-up date	Freeze-up duration (days) 2013-2014	Freeze-up date	Break-up date	Freeze-up duration (days) 2014-2015

14

	2013-204	2013-2014		2014-2015	2014-2015	
WRF-Ctrl	146(-57)	261(-37)	115	152(-44)	267(-35)	115
WRF-FLake	**202(-1)**	307(+9)	105	202(+6)	**303(+1)**	**101**
WRF-CLake	192(-11)	**294(-4)**	**102**	**194(-2)**	276(-26)	82
MODIS	203(19th JAN)	298(24th APR)	95	196(12th JAN)	302(28th APR)	106

350
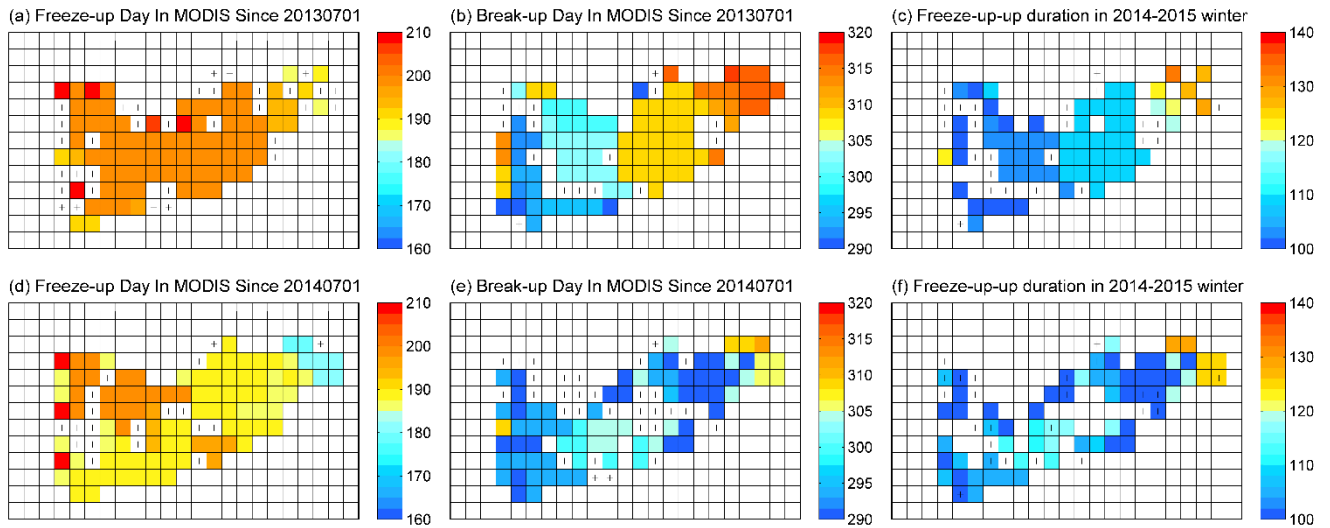
Figure 6: Spatial distribution of freeze-up date (left), break-up date (middle), and freeze-up duration (right) at Nam Co derived from MODIS in the period of (a-c) 2013-2014 and (d-f) 2014-2015. The cross marks denote lake grid points with missing observations in MODIS.

355

Figure 6 shows the spatial distribution of freeze-up date, break-up date, and freeze-up duration derived from MODIS data in the winter of 2013-2014 and 2014-2015. There are missing values at considerable grid points due to the missing LST observation by MODIS. Generally, the east Nam Co shows a little earlier freeze-up time than the west, while the west Nam Co obvious shows much earlier break-up time than the east. As a result, the east Nam Co has longer freeze-up duration. The freeze-up date, break-up date, and freeze-up duration in MODIS will be used to quantitatively evaluate the simulations. The

15

inconsistencies in spatial distribution of these three variables between simulations and MODIS will be discussed in the next section.

Figure 7 shows the spatial distribution of freeze-up date in each simulation. WRF-Ctrl predicted early freeze-up, while both revised models are consistent and show late freeze-up in eastern Nam Co, early freeze-up in the middle of the lake for winters of 2013-2014 and 2014-2015. Additionally, WRF-FLake predicted slightly later freeze-up date than WRF-CLake. Figure 8 shows the spatial distribution of biases in freeze-up date in each simulation derived from WRF-Ctrl, WRF-Flake, and WRF-CLake runs minus MODIS. A positive value indicates a later freeze-up, while a negative value indicates an earlier freeze-up. Compared with MODIS, WRF-Ctrl predicted systematically too early freeze-up date by more than 30 days, while the WRF-FLake and WRF-CLake runs show considerable smaller biases within ±20 days, with negative biases over the mid-western lake and positive biases over the eastern lake except for freeze-up date in 2014-2015 in the WRF-FLake. Generally, the variability of the biases is low (blue text in Figure 8), indicating a reliable quantification.
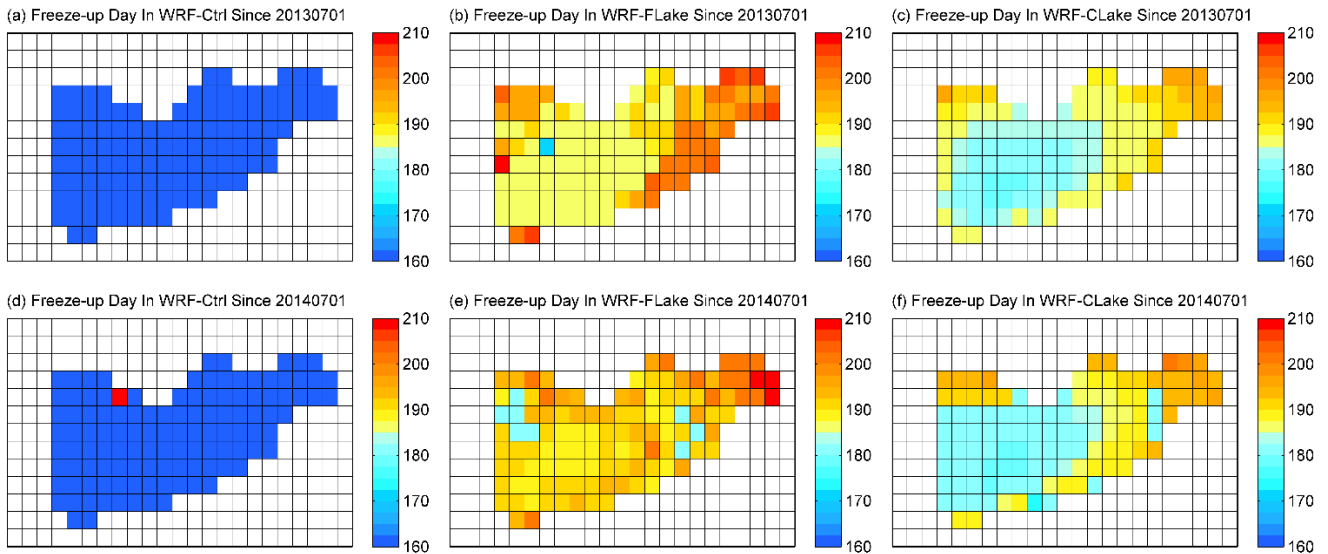

Figure 7: Spatial distribution of freeze-up date at Nam Co in each simulation in the winters of (a-c) 2013-2014 and (d-f) 2014-2015. The colour indicates the number of days since 1st July in the corresponding year.
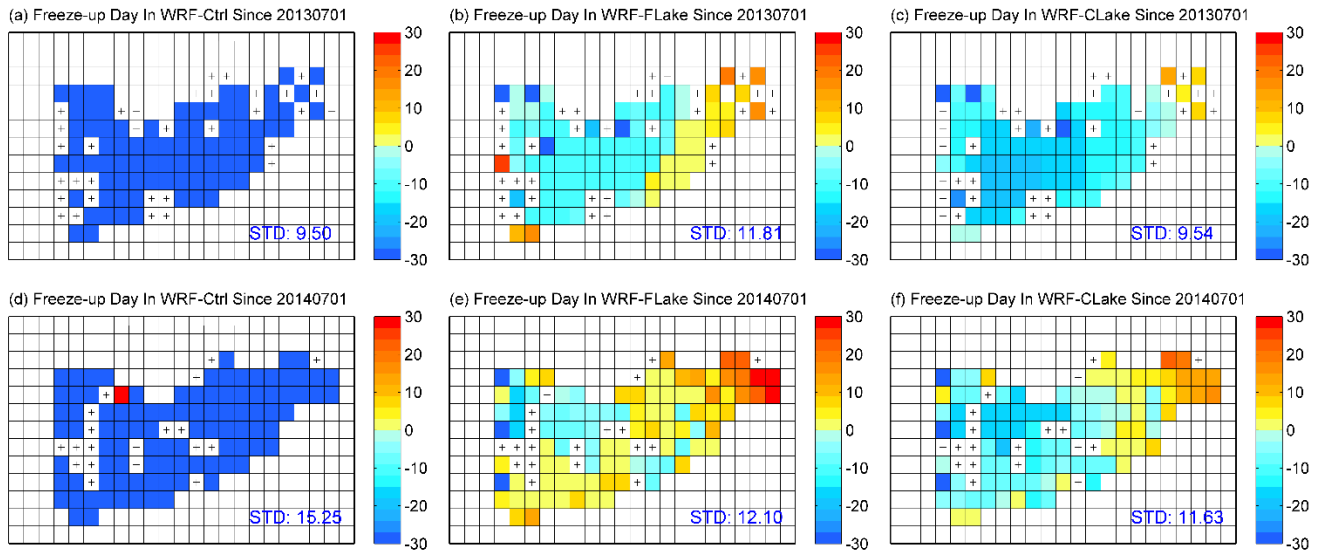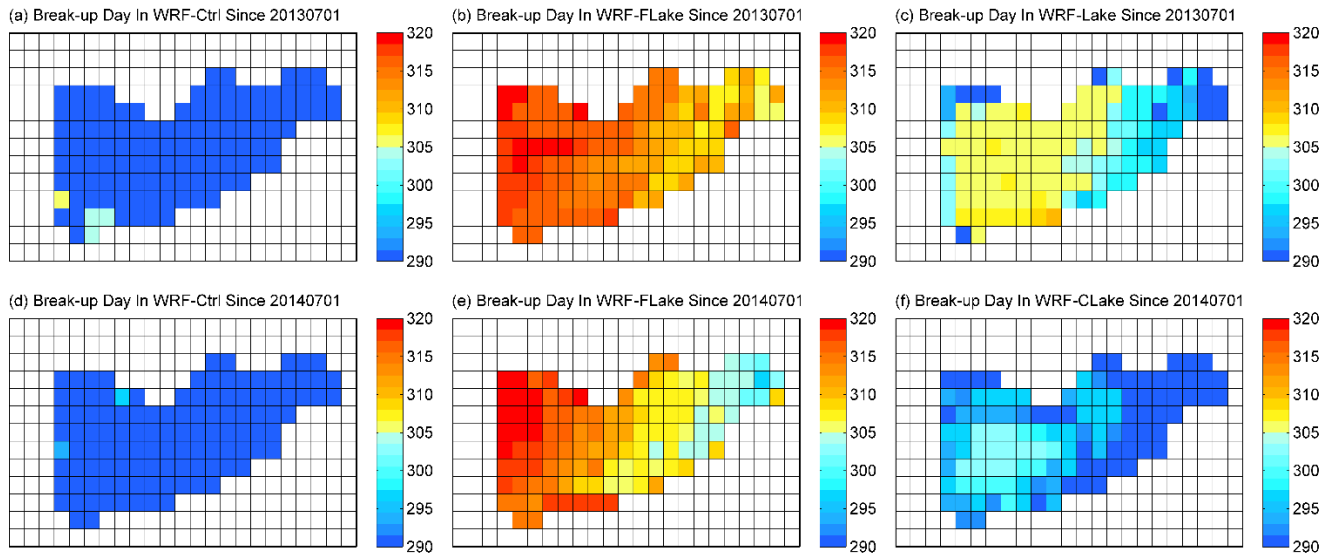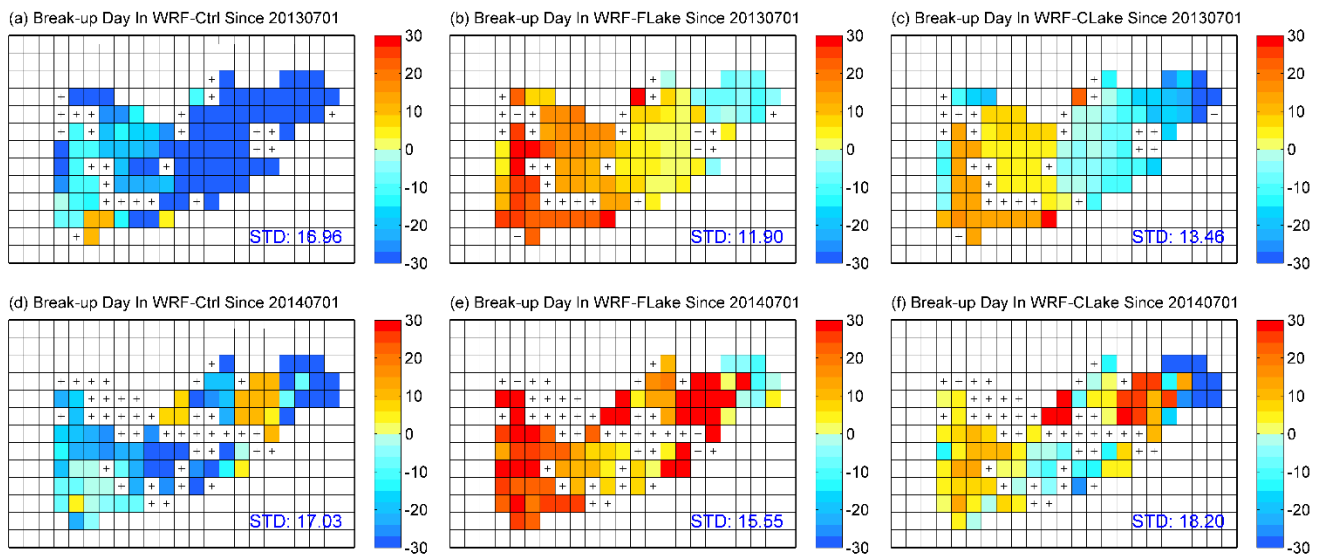
16

Figure 8: Spatial distribution of biases (days) in freeze-up date at Nam Co in each simulation in the winters of (a-c) 2013-2014 and (d-f) 2014-2015. The biases are derived from WRF-Ctrl, WRF-Flake, and WRF-CLake runs minus MODIS. The cross marks denote lake grid points with missing observations in MODIS.

Figure 9 shows the spatial distribution of break-up date in each simulation. WRF-Ctrl predicted early break-up, while both revised models show late break-up in western Nam Co, and early break-up in the middle for both springs of 2014 and 2015. The too early break-up in WRF-Ctrl could be associated with the too thin ice during freezing, and the ice-water phase change requires much less energy and thus a short time. Additionally, WRF-FLake predicted a slightly later break-up date than WRF-CLake, which could be associated with the lake ice thickness in both runs. WRF-FLake has thicker ice during freezing and more energy is required for the ice-water phase change and thus it takes a longer time. Figure 10 shows the spatial distribution of biases in break-up date in each simulation. Compared with MODIS, WRF-Ctrl predicted systematically too early break-up date by approximately 10-20 days, while the WRF-FLake and WRF-CLake runs show late break-up dates over the mid-western lake (more than 20 days and 0-10 days respectively) and early break-up dates over the eastern lake (-10-0 days and smaller than -20 days respectively). Generally, the variability of the biases in break-up date (blue text in Figure 10) is a little higher than that in freeze-up date, which could be due to more missing values in MODIS break-up date.

17

Figure 9: Spatial distribution of break-up date at Nam Co in each simulation in the spring of (a-c) 2014 and (d-f) 2015, colour indicates the number of days since 1ˢᵗ July.

Figure 10: Spatial distribution of biases (days) in break-up date at Nam Co in each simulation in the spring of (a-c) 2014 and (d-f) 2015, colour indicates the number of days since 1ˢᵗ July. The biases are derived from WRF-Ctrl, WRF-Flake, and WRF-CLake runs minus MODIS. The cross marks denote lake grid points with missing observations in MODIS.

18

Figure 11 shows the spatial distribution of freeze-up duration simulated by the two models. All models predicted the longest ice duration in the middle west of Nam Co, with WRF-Ctrl having the longest ice duration and WRF-FLake having a slightly longer freeze-up duration than that of WRF-CLake. The differences in the latter two runs could be associated with the differences in the parameterizations of shortwave processes when lake ice exists. Generally, the simulated ice duration is longer than 100 days and shorter than 140 days in both revised models. Figure 12 shows the spatial distribution of biases in freeze-up duration in each simulation. Compared with MODIS, all the models show longer freeze-up durations over the mid-western lake (approximately 10-20 days) and shorter freeze-up durations over the eastern corner of lake Nam Co (approximately -20 --10 days). The too long freeze-up duration in WRF-Ctrl could be associated with the too early freeze-up dates, while the too long freeze-up duration in WRF-FLake and WRF-CLake could be associated with the too late break-up dates. Generally, the variability of the biases in freeze-up duration (blue text in Figure 10) is much higher than those in freeze-up date and break-up date, which is obviously due to more missing values in MODIS when subtracting the two.
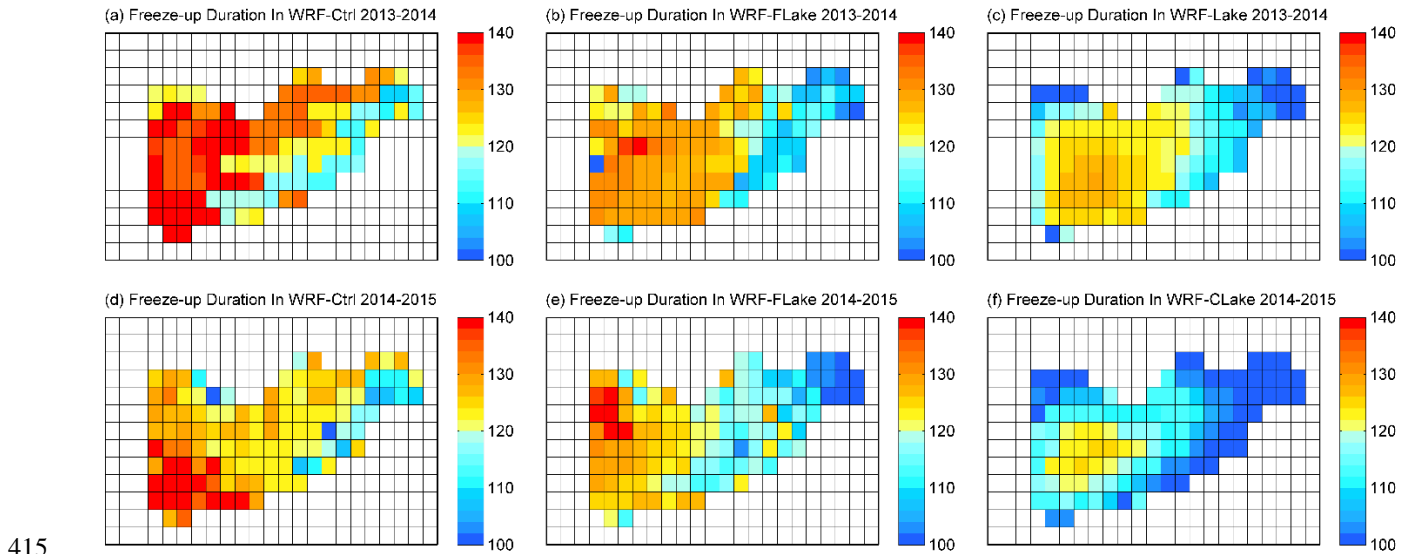

Figure 11: Spatial distribution of freeze-up duration in each simulation in the periods of (a-c) 2013-2014 and (d-f) 2014-2015, colour indicates the number of days during freeze-up.
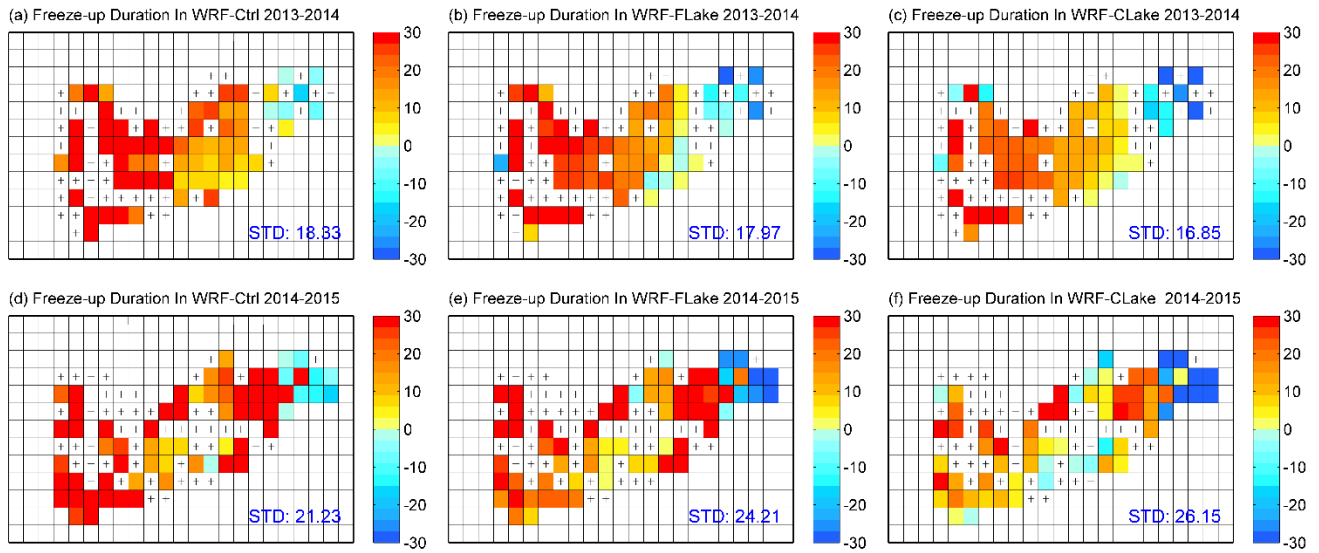
19

Figure 12: Spatial distribution of biases (days) in freeze-up duration in each simulation in the periods of (a-c) 2013-2014 and (d-f) 2014-2015, colour indicates the number of days during freeze-up. The biases are derived from WRF-Ctrl, WRF-Flake, and WRF-CLake runs minus MODIS. The cross marks denote lake grid points with missing observations in MODIS.
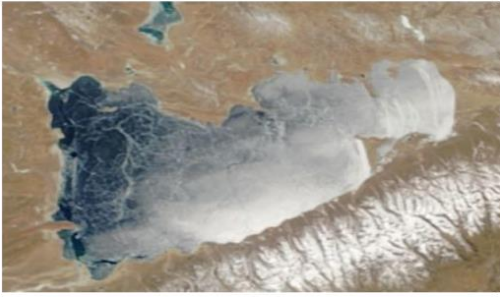
5 Discussion

The above evaluations demonstrate that with revisions of key parameters and improvements of key parametrizations, associated with surface turbulent heat fluxes during ice-free period and associated with solar radiation transfer during ice-on period, the updated model versions can significantly improve the simulation of ice phenology through a better representation of lake energy processes. These improvements are observation and physics based, which is more reasonable and more universal than using artificial scaling method (i.e. When calculating the sensible heat and latent heat, multiply by a constant) as in *Zhou et al.* [2023]. For example, both WRF-FLake and WRF-CLake models are improved by the same parameterization of water surface roughness length, demonstrating the universality of this scheme as described in Eq. (4)-(5). Therefore, the current work provides a better model version for weather and climate simulations over alpine lake regions. Nevertheless, there might still be large uncertainties caused by the limitations of models' abilities in depicting some physical processes, which will be discussed in this section.

For freeze-up date, in both periods in 2013-2014 and 2014-2015, MODIS shows early freeze-up in the east of Nam Co (Figure 6a, 6d), while models show early freeze-up in the middle-west (Figure 7). The identical lake depth inevitably causes uncertainties in simulating the freeze-up date. Shallow water grid points freeze-up earlier than deep water grid points due to less water and low heat capacity per unit area. Essentially, both lake models are one-dimensional models, and thus we speculate that the mismatch between the model and observation might also be associated with the lake water circulation that

cannot be represented in the one-dimension lake models. In cold seasons, the TP is dominated by prevailing westerlies. Before freeze-up, the wind blowing effect may lead to surface cooling water moving to the east and deep warm water moving to the west. A three-dimensional lake model is expected to solve this problem by depicting the horizontal lake water circulation as demonstrated in previous studies [*White et al.,* 2012; *Wu et al.,* 2021]. Nevertheless, a one-dimensional lake model is still commonly used in climate models when simulating atmosphere-lake processes, such as the widely used CESM [*Oleson et al.,* 2010], and COSMO [*Steppeler et al.,* 2003], which highlights the importance of the current work.

For break-up date, in both periods in 2013-2014 and 2014-2015, MODIS shows early break-up in the west (Figure 6b, 6e) while models show early break-up in eastern Nam Co (Figure 9). The freeze-up time in the models may play a role, because early freeze-up grid points may accumulate thicker ice and vice versa for late freeze-up grid points. Additionally, uncertainties associated with snow cover at the lake ice surface play an important role through shortwave-albedo processes, as highlighted by *Li et al.* [2018] for offline models. In the simulations, there are nearly no snow cover (not shown). However, Figure 13a and 13b show that a considerable amount of snow covers the lake surface with inhomogeneous distribution from the west to the east of lake Nam Co, when looking at the images from the Earth Observing System Data and Information System (EOSDIS). Nearly no snow covers the west and a considerable amount of snow exists over the east. More snow can lead to a high albedo and less shortwave absorption at the surface and thus have a cooling effect, which will delay ice melting. This contrast in snow cover between the model and observations is consistent and may partly explain the contrast in the spatial patterns of the lake break-up date over Nam Co. In the simulations, nearly no precipitation and snow cover is predicted over the lake ice during freeze-up (not shown). Frozen and smooth surfaces are not favourable for triggering atmospheric convection and snowfall. Therefore, we speculate that the snow covers at lake ice surface, as shown in the sky view images, might be associated with grid-scale snow dynamic processes like blowing snow during snowfall (as snowflake descent) and after snowfall (at land/lake surface). Previous studies have also demonstrated that snow redistribution by wind and associated changes in depth and density of the snow pack contribute to variations in ice thickness [*Brown and Duguay,* 2010; 2011]. With rough surfaces such as bare ground or vegetated land, the scale of blowing snow might be limited to a small scale and can be parameterized by a scheme such as the one introduced by *Xie et al.* [2019]. In contrast, for a smooth surface, such as the ice surface in the current work, the scale of blowing snow can be much larger. However, such processes are not included in the model version used in current study and the applicability of such a scheme needs to be further investigated. Furthermore, lakes generally have lower elevations than the surrounding land and are beneficial for snow accumulation, especially during snowfall. Noting that the accurate simulation of precipitation over the complex terrain has long been a challenging issue, i.e. the precipitation in TP can be overestimated by more than 50% in climate models and even reanalysis data [*Gao et al.,* 2015; *Su et al.,* 2013], the simulated over lake snow fall will also bring large uncertainties in modeling the lake surface albedo and thus can influence the lake ice phenology as also demonstrated in previous study over high latitude lakes [*Fujisaki-Manome et al.,* 2020].

Figure 13: Satellite sky view images from EOSDIS Worldview on typical lake ice-on days in (a) 20140315 and (b) 20150226 (right).

475 Additionally, other lake processes can also bring uncertainties in simulating the lake ice phenology. For example, during ice-covered period, the shortwave radiation absorbed by lake water under ice can increase the water temperature to more than the freezing point [*Kirillin et al.*, 2021; *La et al.*, 2021; *Wang et al.*, 2022] and delay ice melting by temporally storing the energy in water instead of being used immediately for ice melting. These uncertainties in describing lake-related processes bring considerable inconsistencies between models and observations associated with ice phenology. Simultaneously, they
480 also bring great challenges in model applications and developments, especially for deep alpine lake regions.

6 Summary and remarks

In this study, the WRF model coupled with two lake models, the FLake model and the default simplified CLM lake model (namely WRF-FLake and WRF-CLake, respectively), have been applied to simulate lake ice phenology in a typical alpine lake located in the central TP. With improvements of momentum, hydraulic and thermal roughness length parameterizations,
485 both the WRF-FLake and the WRF-CLake models reasonably simulated the lake water temperature compared with MODIS and station observations. Water temperature represents the lake energy storage, and therefore, the lake freeze-up date in both models was reasonably simulated compared with MODIS. With improvements of key parameterizations associated with the shortwave radiation transfer, both the WRF-FLake and the WRF-CLake models generally simulated the lake break-up date

22

well. Compared with WRF coupled with the default lake model, the simulation of lake ice phenology was significantly
490   improved by WRF coupled to both of the improved lake models. Therefore, we expect that the main results and findings of
this work can provide a good reference when simulating lake ice phenology by climate models, especially for the alpine lake.
However, considerable errors still exist in simulating the spatial patterns of freeze-up and break-up dates. These errors could
come from the disadvantages of the model in representing some key lake physics such as nonuniform lake depth, lake water
circulation, shortwave heating effect on water underneath lake ice, and atmospheric processes such as grid-scale blowing
495   snow, indicating that more substantial work is required to improve the lake physical processes in climate models.
Nevertheless, our work can provide a better model version compared with the default WRF model and the discussions are
expected to provide new implications for improving lake ice associated processes in coupled atmosphere-lake models in the
future.

Code and data availability

500   The model code and simulation data is available online at https://doi.org/10.17632/bpjcbdkj4c.1.

Author contributions

Author contributions: Conceptualization: Xu Zhou and Binbin Wang; Data curation: Xu Zhou and Lazhu; Formal analysis,
Validation and Visualization: Xu Zhou; Funding acquisition: Xu Zhou, Binbin Wang, Lazhu and Kun Yang; Supervision:
Kun Yang; Roles/Writing - original draft: Xu Zhou and Binbin Wang; and Writing - review & editing: All authors.

505   **Competing interests**

The authors declare that there are no conflicts of interest.

References

Brown, L.C. and Duguay, C.R.: The response and role of ice cover in lake-climate interactions. Prog Phys Geog 34(5), 671-
515   704, 2010.
Brown, L.C. and Duguay, C.R.: A comparison of simulated and measured lake ice thickness using a Shallow Water Ice
Profiler. Hydrol Process 25(19), 2932-2941, 2011.

Charusombat, U., Fujisaki-Manome, A., Gronewold, A.D., Lofgren, B.M., Anderson, E.J., Blanken, P.D., Spence, C., Lenters, J.D., Xiao, C.L., Fitzpatrick, L.E. and Cutrell, G.: Evaluating and improving modeled turbulent heat fluxes across the North American Great Lakes. Hydrol Earth Syst Sc 22(10), 5559-5578, 2018.

Dai, Y., Wei, N., Huang, A., Zhu, S., Shangguan, W., Yuan, H., Zhang, S., and Liu, S.: The lake scheme of the Common Land Model and its performance evaluation, Chinese Science Bulletin, 63(28-29), 3002-3021, doi:10.1360/N972018-00609, 2018.

Dai, Y. F., Wang, L., Yao, T. D., Li, X. Y., Zhu, L. J., and Zhang, X. W.: Observed and Simulated Lake Effect Precipitation Over the Tibetan Plateau: An Initial Study at Nam Co Lake, J Geophys Res-Atmos, 123(13), 6746-6759, doi:10.1029/2018jd028330, 2018.

Deacu, D., Fortin, V., Klyszejko, E., Spence, C. and Blanken, P.D.: Predicting the Net Basin Supply to the Great Lakes with a Hydrometeorological Model. J Hydrometeorol 13(6), 1739-1759, 2012.

Dee, D. P., et al.: The ERA-Interim reanalysis: configuration and performance of the data assimilation system, Quarterly Journal of the Royal Meteorological Society, 137(656), 553-597, doi:10.1002/qj.828, 2011.

Dudhia, J.: Numerical Study of Convection Observed during the Winter Monsoon Experiment Using a Mesoscale Two-Dimensional Model, J Atmos Sci, 46(20), 3077-3107, doi:10.1175/1520-0469(1989)046<3077:Nsocod>2.0.Co;2, 1989.

Efremova, T. V., and Pal'shin, N. I.: Ice Phenomena Terms on the Water Bodies of Northwestern Russia, Russ Meteorol Hydro+, 36(8), 559-565, doi:10.3103/S1068373911080085, 2011.

Fujisaki-Manome, A., Anderson, E.J., Kessler, J.A., Chu, P.Y., Wang, J. and Gronewold, A.D.: Simulating Impacts of Precipitation on Ice Cover and Surface Water Temperature Across Large Lakes. J Geophys Res-Oceans 125(5), 2020.

Gu, H. P., Jin, J. M., Wu, Y. H., Ek, M. B., and Subin, Z. M.: Calibration and validation of lake surface temperature simulations with the coupled WRF-CLake model, Climatic Change, 129(3-4), 471-483, doi:10.1007/s10584-013-0978-y, 2015.

Guo, Y. H., Zhang, Y. S., Ma, N., Song, H. T., and Gao H. F.: Quantifying Surface Energy Fluxes and Evaporation over a Significant Expanding Endorheic Lake in the Central Tibetan Plateau, J Meteorol Soc Jpn, 94(5), 453-465, doi:10.2151/jmsj.2016-023, 2016.

Huang, A., Lazhu, Wang, J., Dai, Y., Yang, K., Wei, N., Wen, L., Wu, Y., Zhu, X., Zhang, X., and Cai, S.: Evaluating and Improving the Performance of Three 1-D Lake Models in a Large Deep Lake of the Central Tibetan Plateau, J Geophys Res-Atmos, 124(6), 3143-3167, doi:10.1029/2018jd029610, 2019.

Huang, W. F., Cheng, B., Zhang, J. R., Zhang, Z., Vihma, T., Li, Z. J., and Niu, F. J.: Modeling experiments on seasonal lake ice mass and energy balance in the Qinghai-Tibet Plateau: a case study, Hydrol Earth Syst Sc, 23(4), 2173-2186, doi:10.5194/hess-23-2173-2019, 2019.

Huang, W. F., Zhao, W., Zhang, C., Lepparanta, M., Li, Z. J., Li, R., and Lin, Z. J.: Sunlight penetration dominates the thermal regime and energetics of a shallow ice-covered lake in arid climate, Cryosphere, 16(5), 1793-1806, doi:10.5194/tc-16-1793-2022, 2022.

24

Janjic, Z.: Nonsingular implementation of the Mellor- Yamada level 2.5 scheme in the NCEP mesoscale model. National Centers for Environmental Prediction Office, Tech. Rep., 437, 2001.

Kirillin, G., Leppäranta, M., Terzhevik, A., Granin, N., Bernhardt, J., Engelhardt, C., Efremova, T., Palshin, N.,

555   Sherstyankin, P., Zdorovennova, G., and Zdorovennov, R.: Physics of seasonally ice-covered lakes: a review, Aquat Sci, 74(4), 659-682, doi:10.1007/s00027-012-0279-y, 2012.

Kirillin, G. B., Shatwell, T., and Wen, L. J.: Ice-Covered Lakes of Tibetan Plateau as Solar Heat Collectors, Geophys Res Lett, 48(14), doi:10.1029/2021GL093429, 2021.

La, Z., Yang, K., Qin, J., Hou, J. Z., Lei, Y. N., Wang, J. B., Huang, A. N., Chen, Y. Y., Ding, B. H., and Li, X.: A Strict

560   Validation of MODIS Lake Surface Water Temperature on the Tibetan Plateau, Remote Sens-Basel, 14(21), doi:ARTN 545410.3390/rs14215454, 2022.

La, Z., Yang, K., Wang, J. B., Lei, Y. B., Chen, Y. Y., Zhu, L. P., Ding, B. H., and Qin, J.: Quantifying evaporation and its decadal change for Lake Nam Co, central Tibetan Plateau, J Geophys Res-Atmos, 121(13), 7578-7591, doi:10.1002/2015jd024523, 2016.

565   Lazhu, Yang, K., Hou, J. Z., Wang, J. B., Lei, Y. B., Zhu, L. P., Chen, Y. Y., Wang, M. D., and He, X. G.: A new finding on the prevalence of rapid water warming during lake ice melting on the Tibetan Plateau, Sci Bull, 66(23), 2358-2361, doi:10.1016/j.scib.2021.07.022, 2021.

Lei, Y. B., Yang, K., Wang, B., Sheng, Y. W., Bird, B. W., Zhang, G. Q., and Tian, L. D.: Response of inland lake dynamics over the Tibetan Plateau to climate change, Climatic Change, 125(2), 281-290, doi:10.1007/s10584-014-1175-3, 2014.

570   Lei, Y. B., Yao, T. D., Bird, B. W., Yang, K., Zhai, J. Q., and Sheng, Y. W.: Coherent lake growth on the central Tibetan Plateau since the 1970s: Characterization and attribution, J Hydrol, 483, 61-67, doi:10.1016/j.jhydrol.2013.01.003, 2013.

Lei, Y.B., Yao, T.D., Yang, K., Bird, B.W., Tian, L.D., Zhang, X.W., Wang, W.C., Xiang, Y., Dai, Y.F., Lazhua, Zhou, J., Wang, L.: An integrated investigation of lake storage and water level changes in the Paiku Co basin, central Himalayas, J Hydrol, 562, 599-608, doi:10.1016/j.jhydrol.2018.05.040, 2018.

575   Li, X.Y., Ma, Y.J., Huang, Y.M., Hu, X., Wu, X.C., Wang, P., Li, G.Y., Zhang, S.Y., Wu, H.W., Jiang, Z.Y., Cui, B.L., & Liu, L.: Evaporation and surface energy budget over the largest high-altitude saline lake on the Qinghai-Tibet Plateau, J Geophys Res-Atmos, 121(18), 10470-10485, doi:10.1002/2016jd025027, 2016.

Li, Z. G., Ao, Y. H., Lyu, S., Lang, J. H., Wen, L. J., Stepanenko, V., Meng, X. H., and Zhao, L.: Investigation of the ice surface albedo in the Tibetan Plateau lakes based on the field observation and MODIS products, J Glaciol, 64(245), 506-516,

580   doi:10.1017/jog.2018.35, 2018).

Li, Z. G., Lyu, S. H., Wen, L. J., Zhao, L., Ao, Y. H., and Meng X. H.: Study of freeze-thaw cycle and key radiation transfer parameters in a Tibetan Plateau lake using LAKE2.0 model and field observations, J Glaciol, 67(261), 91-106, doi:10.1017/jog.2020.87, 2021.

Ma, X. G., Yang, K., La, Z., Lu, H., Jiang, Y. Z., Zhou, X., Yao, X. N., and Li, X.: Importance of Parameterizing Lake
Surface and Internal Thermal Processes in WRF for Simulating Freeze Onset of an Alpine Deep Lake, J Geophys Res-
Atmos, 127(18), doi:10.1029/2022JD036759, 2022.

Mellor, G. L., and Yamada, T.: Hierarchy of Turbulence Closure Models for Planetary Boundary-Layers, J Atmos Sci, 31(7),
1791-1806, doi:10.1175/1520-0469(1974)031<1791:Ahotcm>2.0.Co;2, 1974.

Mironov, D.: Parameterization of Lakes in Numerical Weather Prediction. Description of a Lake Model.Rep, 2008.

Mlawer, E. J., Taubman, S. J., Brown, P. D., Iacono, M. J., and Clough, S. A.: Radiative transfer for inhomogeneous
atmospheres: RRTM, a validated correlated-k model for the longwave, J Geophys Res-Atmos, 102(D14), 16663-16682,
doi:10.1029/97jd00237, 1997.

Niu, G. Y., Yang, Z. L., Mitchell, K. E., Chen, F., Ek, M. B., Barlage, M., Longuevergne, L., Manning, K., Niyogi, D.,
Tewari, M., and Xia, Y.: The community Noah land surface model with multiparameterization options (Noah-MP): 1. Model
description and evaluation with local-scale measurements, J Geophys Res-Atmos, 116, doi:10.1029/2010jd015139, 2011.

Skamarock, W. C., Klemp, J. B., Gill, D. O., Barker, D. M., Duda, M. G., Huang, X., Wang, W., and Powers, J. G.: A
description of the advanced research WRF model version 3Rep., National Center for Atmospheric Research, National Center
for Atmospheric Research: Boulder, CO, USA, 145, 2008.

Oleson, K. W., Lawrence, D. M., Bonan, G. B., Flanner, M. G., Kluzek, E., Lawrence, P. J., … Zeng, X.: Technical
Description of version 4.0 of the Community Land Model (CLM) (No. NCAR/TN-478+STR). University Corporation for
Atmospheric Research. doi:10.5065/D6FB50WZ, 2010.

Steppeler, J., Doms, G., Schättler, U., Bitzer, H., Gassmann, A., Damrath, U., and Gregoric, G.: Meso-gamma scale forecasts
using the nonhydrostatic model LM, Meteorol. Atmos. Phys., 82, 75-96, 2003.

Su, D. S., Wen, L. J., Gao, X. Q., Lepparanta, M., Song, X. Y., Shi, Q. Q., and Kirillin, G.: Effects of the Largest Lake of the
Tibetan Plateau on the Regional Climate, J Geophys Res-Atmos, 125(22), doi:10.1029/2020JD033396, 2020.

Thompson, G., Field, P. R., Rasmussen, R. M., and Hall, W. D.: Explicit Forecasts of Winter Precipitation Using an
Improved Bulk Microphysics Scheme. Part II: Implementation of a New Snow Parameterization, Mon Weather Rev, 136(12),
5095-5115, doi:10.1175/2008mwr2387.1, 2008.

Wan, Z., Hook, S., and Hulley, G.: MYD11C3 MODIS/Aqua Land Surface Temperature/Emissivity Monthly L3 Global
0.05Deg CMG V006 [Dataset], edited, doi:10.5067/MODIS/MYD11C3.006, 2015.

Wang, B. B., Ma, Y. M., Wang, Y., Su, Z. B., and Ma, W.: Significant differences exist in lake-atmosphere interactions and
the evaporation rates of high-elevation small and large lakes, J Hydrol, 573, 220-234, doi:10.1016/j.jhydrol.2019.03.066,
2019.

Wang, J. B.: Water temperature observation data at Nam Co Lake in Tibet (2011-2014), edited by National Tibetan Plateau
Data Center, National Tibetan Plateau Data Center, doi:10.11888/Hydro.tpdc.270332, 2020.

Wang, J. B., Huang, L., Ju, J. T., Daut, G., Wang, Y., Ma, Q. F., Zhu, L. P., Haberzettl, T., Baade, J., andMausbacher, R.: Spatial and temporal variations in water temperature in a high-altitude deep dimictic mountain lake (Nam Co), central Tibetan Plateau, J Great Lakes Res, 45(2), 212-223, doi:10.1016/j.jglr.2018.12.005, 2019.

620 Wang, J. B., Zhu, L. P., Daut, G., Ju, J. T., Lin, X., Wang, Y., and Zhen X. L.:, Investigation of bathymetry and water quality of Lake Nam Co, the largest lake on the central Tibetan Plateau, China, Limnology, 10(2), 149-158, doi:10.1007/s10201-009-0266-8, 2009.

Wang, M. X., Wen, L. J., Li, Z. G., Lepparanta, M., Stepanenko, V., Zhao, Y. X., Niu, R. J., Yang, Y. Y., and Kirillin, G.: Mechanisms and effects of under-ice warming water in Ngoring Lake of Qinghai-Tibet Plateau, Cryosphere, 16(9), 3635-3648, doi:10.5194/tc-16-3635-2022, 2022.

625 Wen, L. J., Lyu, S. H., Kirillin, G., Li, Z. G., and Zhao L: Air-lake boundary layer and performance of a simple lake parameterization scheme over the Tibetan highlands, Tellus A, 68, doi:10.3402/tellusa.v68.31091, 2016).

White, B., Austin, J. and Matsumoto, K.: A three-dimensional model of Lake Superior with ice and biogeochemistry. J Great Lakes Res 38(1), 61-71, 2012.

Wu, Y., Huang, A.N., Lu, Y.Y., Fujisaki-Manome, A., Zhang, Z.Q., Dai, X.L. and Wang, Y.: Application of a Three-630 Dimensional Coupled Hydrodynamic-Ice Model to Assess Spatiotemporal Variations in Ice Cover and Underlying Mechanisms in Lake Nam Co, Tibetan Plateau, 2007-2017. J Geophys Res-Atmos 128(24), 2023

Wu, Y., Huang, A. N., Lu, Y. Y., Lazhu, Yang, X. Y., Qiu, B., Zhang, Z. Q., and Zhang, X. D.: Numerical Study of the Thermal Structure and Circulation in a Large anal Deep Dimictic Lake Over Tibetan Plateau, J Geophys Res-Oceans, 126(10), doi:10.1029/2021JC017517, 2021.

635 Wu, Y., Huang, A. N., Yang, B., Dong, G. T., Wen, L. J., Lazhu, Zhang, Z., Fu, Z., Zhu, X., Zhang, X., Cai, S.: Numerical study on the climatic effect of the lake clusters over Tibetan Plateau in summer, Clim Dynam, 53(9-10), 5215-5236, doi:10.1007/s00382-019-04856-4, 2019.

Xie, Z., Hu, Z., Ma, Y., Sun, G., Gu, L., Liu, S., Wang, Y., Zheng, H., and Ma, W.: Modeling Blowing Snow Over the Tibetan Plateau With the Community Land Model: Method and Preliminary Evaluation, Journal of Geophysical 640 Research: Atmospheres, 124(16), 9332-9355, doi:10.1029/2019JD030684, 2019.

Xu, X. D., Lu, C. G., Shi, X. H., and Gao, S. T.: World water tower: An atmospheric perspective, Geophys Res Lett, 35(20), doi:10.1029/2008gl035867, 2008.

Yang, X. Y., Wen, J., Huang, A. N., Lu, Y. Q., Meng, X. H., Zhao, Y., Wang, Y. R., and Meng, L. X.: Short-Term Climatic Effect of Gyaring and Ngoring Lakes in the Yellow River Source Area, China, Front Earth Sc-Switz, 9, 645 doi:10.3389/feart.2021.770757, 2022.

Yang, Z. L.: The community Noah land surface model with multiparameterization options (Noah-MP): 2. Evaluation over global river basins, J Geophys Res-Atmos, 116, doi:10.1029/2010jd015140, 2011.

Yao, X. N., Yang, K., Letu, H., Zhou, X, Wang, Y., Ma, X., Lu, H. and La, Z.: Observation and Process Understanding of Typical Cloud Holes Above Lakes Over the Tibetan Plateau, Journal of Geophysical Research: Atmospheres, 128(13),

650   e2023JD038617, doi:10.1029/2023JD038617, 2023.

Yao, X. N., Yang, K., Zhou, X., Wang, Y., Lazhu, Chen, Y. Y., and Lu, H: Surface friction contrast between water body and land enhances precipitation downwind of a large lake in Tibet, Clim Dynam, 56(7-8), 2113-2126, doi:10.1007/s00382-020-05575-x, 2021.

Zhang, G. Q., Luo, W., Chen, W. F., and Zheng, G. X.: A robust but variable lake expansion on the Tibetan Plateau, Sci Bull,

655   64(18), 1306-1309, doi:10.1016/j.scib.2019.07.018, 2019.

Zhang, G. Q., Yao, T. D., Xie, H. J., Qin, J., Ye, Q. H., Dai, Y. F., and Guo, R. F.: Estimating surface temperature changes of lakes in the Tibetan Plateau using MODIS LST data, J Geophys Res-Atmos, 119(14), 8552-8567, doi:10.1002/2014jd021615, 2014.

Zhang, G., Yao, T., Xie, H., Yang, K., Zhu, L., Shum, C. K., Bolch, T., Yi, S., Allen, S., Jiang, L., Chen, W., and Ke, C.:

660   Response of Tibetan Plateau lakes to climate change: Trends, patterns, and mechanisms, Earth-Sci Rev, 208, doi:10.1016/j.earscirev.2020.103269, 2020.

Zhao, Z. Z., Huang, A. N., Ma, W. Q., Wu, Y., Wen, L. J., Lazhu, and Gu, C. L.: Effects of Lake Nam Co and Surrounding Terrain on Extreme Precipitation Over Nam Co Basin, Tibetan Plateau: A Case Study, J Geophys Res-Atmos, 127(10), doi:10.1029/2021JD036190, 2022.

665   Zhou, X., Beljaars, A., Wang, Y., Huang, B., Lin, C., Chen, Y., and Wu, H.: Evaluation of WRF Simulations With Different Selections of Subgrid Orographic Drag Over the Tibetan Plateau, J Geophys Res-Atmos, 122(18), 9759-9772, doi:10.1002/2017jd027212, 2017.

Zhou, X., Lazhu, Yao, X., and Wang, B.: Understanding two key processes associated with alpine lake ice phenology using a coupled atmosphere-lake model, Journal of Hydrology: Regional Studies, 46, 101334, doi:10.1016/j.ejrh.2023.101334, 2023.

670   Zhou, X., Yang, K., Ouyang, L., Wang, Y., Jiang, Y. Z., Li, X., Chen, D. L., and Prein, A.: Added value of kilometer-scale modeling over the third pole region: a CORDEX-CPTP pilot study, Clim Dynam, 57(7-8), 1673-1687, doi:10.1007/s00382-021-05653-8, 2021.